

Electronic and Optical Properties of Ultrawide Bandgap Perovskite Semiconductors via First Principles Calculations

Radi A. Jishi,¹ Robert J. Appleton,² and David M. Guzman^{2, a)}

¹⁾*Department of Physics and Astronomy, California State University, Los Angeles, California 90032, USA*

²⁾*School of Materials Engineering and Birck Nanotechnology Center, Purdue University, West Lafayette, Indiana 47907, USA*

(Dated: 6 February 2022)

Recent research in ultrawide-bandgap (UWBG) semiconductors has focused on traditional materials such as Ga_2O_3 , AlGaN , AlN , cubic BN , and diamond; however some materials exhibiting single perovskite structure have been known to yield bandgaps above 3.4 eV, such as BaZrO_3 . In this work we propose two novel materials to be added to the family of UWBG semiconductors: $\text{Ba}_2\text{CaTeO}_6$ exhibiting a double perovskite structure and $\text{Ba}_2\text{K}_2\text{Te}_2\text{O}_9$ with a triple perovskite structure. Using first principles hybrid functional calculations we predict the bandgaps of all the studied systems to be above 4.5 eV with strong optical absorption in the ultraviolet region. Furthermore, we show that holes have a tendency to get trapped through lattice distortions in the vicinity of oxygen atoms with average trapping energy of 0.25 eV, potentially preventing the enhancement of p -type conductivity through traditional chemical doping.

^{a)}Corresponding Author: davgumo@me.com

Technological developments in electronics, photonics, electro- and photo-chemistry have been based in traditional materials such Ge, Si, and III-Vs compounds¹, all generally characterized by bandgaps under 2.3 eV. However, in the last 10 years the wide bandgap semiconductor InGaN became the second most important material, behind Si², because of its application in solid state lighting³, which has rapidly changed how the world makes use of light sources⁴.

Ultrawide bandgap (UWBG) semiconductors are materials with a bandgap wider than 3.4 eV, the bandgap of GaN. These materials are at the forefront of semiconductor research and will be the building blocks for new devices and applications⁵. Some figures of merit for device performance, such as the Baliga figure of merit⁶ for low-frequency power switches, and the Johnson figure of merit⁷ for high-frequency applications, have a nonlinear dependence on the bandgap. Replacing conventional semiconductors with these UWBG semiconductors in areas such as high-power and RF-electronics, as well as deep-UV optoelectronics, could result in rapid improvements in device performance.

Acceptor doping has been difficult to achieve in UWBG semiconductors mainly due to the tendency of holes to self-trap^{8,9} and the presence of compensating defects. However, it was recently demonstrated that by pinning the Fermi level in AlGaN/AlN away from the valence band edge during epitaxy, it was possible to realize a reduction in the formation energy of substitutional Mg-dopant along with an increase in the formation energy of compensating defects, leading to enhanced p-type doping¹⁰.

Though most of the research on UWBG semiconductors has focused on AlGaN/AlN, diamond, and Ga₂O₃, the domain of UWBG semiconductors is not restricted to those materials. Other materials have also been explored, such as the ternary oxides MgGa₂O₄¹¹ and ZnGa₂O₄¹², the ternary nitrides MgSiN₂ and ZnSiN₂¹³, the alloys α -(AlGa)₂O₃¹⁴, and two-dimensional GaN realized via graphene encapsulation¹⁵.

As technology evolves, pushing the intrinsic performance boundaries of materials to their limits, we face the need to find novel alternative materials to enable the continuation of technological development. Research in the relatively new field of UWBG semiconductors continues to focus on traditional aluminum- and gallium-based materials; however, prototypical structures taken mostly from energy harvesting applications, such as barium-based perovskites, show great potential to be included in the UWBG semiconductors category, bringing a new class of chemistries and structures into the field.

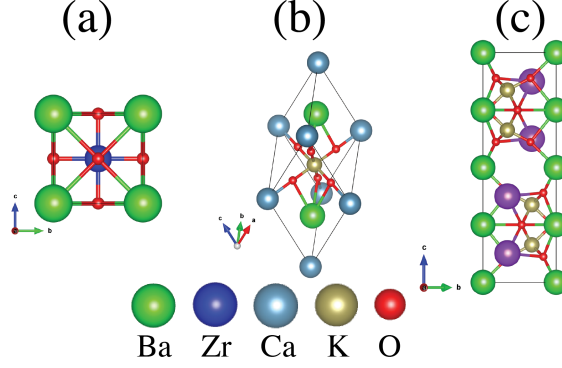


FIG. 1. Primitive cells for (a) simple cubic BaZrO_3 , (b) face-centered cubic $\text{Ba}_2\text{CaTeO}_6$, and (c) hexagonal $\text{Ba}_2\text{K}_2\text{Te}_2\text{O}_9$

In this letter, we use first-principles calculations to study the electronic and optical properties of BaZrO_3 , $\text{Ba}_2\text{CaTeO}_6$, and $\text{Ba}_2\text{K}_2\text{Te}_2\text{O}_9$, three crystals of the perovskite type. Using hybrid functionals, we show that these are UWBG semiconductors with band gaps exceeding 4.9 eV and with significant absorption in the deep-UV region. We also consider the problem of hole self-trapping and calculate the hole self-trap energy.

BaZrO_3 is an ideal perovskite with space group $\text{Pm}\bar{3}\text{m}$ and lattice constant of 4.19 Å¹⁶, figure 1(a). $\text{Ba}_2\text{CaTeO}_6$ is a face-centered cubic double perovskite with space group $\text{Fm}\bar{3}\text{m}$ and lattice constant of 8.3536 Å, figure 1(b); its structure was determined by Fu *et al.*¹⁷ and recently refined by Weil¹⁸. $\text{Ba}_2\text{K}_2\text{Te}_2\text{O}_9$ is a hexagonal triple perovskite with space group $\text{P6}_3/\text{mmc}$ and lattice constants $a = 6.047$ Å and $c = 16.479$ Å, figure 1(c); it has been recently synthesized by Weil¹⁸.

Electronic structure and optical properties calculations are carried out using the all-electron, full potential, linear augmented plane wave method as implemented in the WIEN2k code¹⁹. Each atom is surrounded by a muffin-tin sphere inside which the valence electrons wave function is expanded in spherical harmonics. In the interstitial region outside the muffin-tin spheres, the wave function is expanded in plane waves with a wave vector cutoff K_{max} such that $R_{\text{mt}}K_{\text{max}} = 7$, where R_{mt} is the smallest of the muffin-tin radii. Charge density is Fourier expanded up to $G_{\text{max}} = 12 \text{ Ry}^{1/2}$. The calculations are based on the hybrid-functional HSE06²⁰ potentials.

Our calculations for hole trapping use the HSE06 potential as implemented in the VASP code²¹. Projector augmented wave potentials are used for the interaction between ionic cores

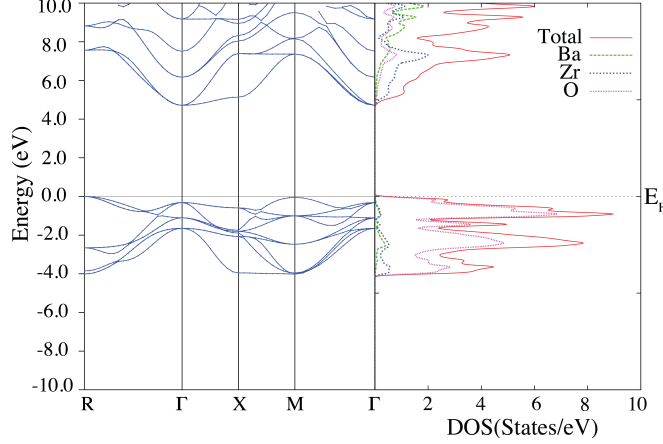


FIG. 2. Left panel: DFT/HSE computed electronic band dispersion of BaZrO₃ crystal along high symmetry directions in the first Brillouin zone. Right panel: Total and partial densities of states for Ba, Zr, and O atoms. The Fermi level has been set to zero matching the top of the valence band.

and valence electrons. To study a small polaron, optimized supercells are used as starting structures. For the cubic BaZrO₃, a 3x3x3 supercell with 135 atoms is adopted, and one special k-point (0.25, 0.25, 0.25) is used to integrate over the Brillouin zone of the supercell. For the fcc double perovskite Ba₂CaTeO₆, a supercell of 80 atoms, obtained by doubling the conventional unit cell, is used, with a 4x4x2 k-mesh. As for the hexagonal triple perovskite Ba₂K₂Te₂O₉, a 2x2x1 supercell with 120 atoms is used, with a k-mesh of 2x2x2. Energy cutoff was set at 400 eV throughout these calculations.

The energy bands and densities of states of the single, double, and triple perovskites, calculated with the HSE06 potential, are shown in figures 2, 3, and 4, respectively. The bandgaps, obtained with the PBE²² and HSE06 potentials are presented in Table I. The calculated bandgap of BaZrO₃, 4.90 eV, is in good agreement with reported experimental value, 4.8-5.3 eV^{23,24}. No experimental values for the bandgap are reported for the double and triple perovskites considered in this work.

In the three crystals considered in this work, the upper valence bands are dominated by O-2p orbitals; these orbitals also contribute in a significant way to the lowest conduction band. Other contributions to the lowest conduction band are made by Zr-4d orbitals in the case of BaZrO₃ and by Te-5s orbitals in the case of the double and triple perovskites.

In figure 5 we present the calculated absorption coefficients and the imaginary parts

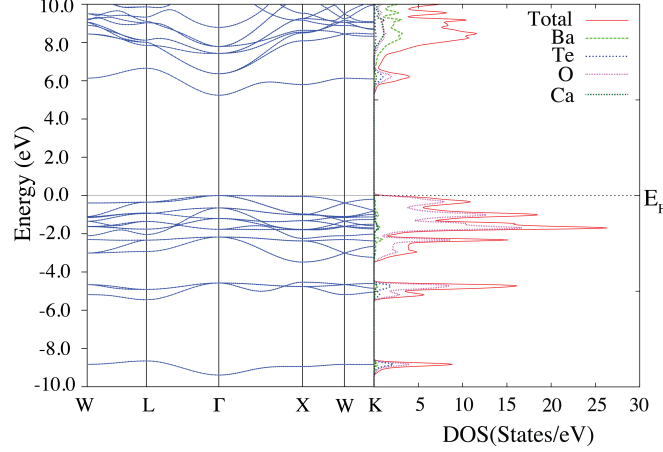


FIG. 3. Left panel: DFT/HSE computed electronic band dispersion of $\text{Ba}_2\text{CaTeO}_6$ crystal along high symmetry directions in the first Brillouin zone. Right panel: Total and partial densities of states for Ba, Te, O, and Ca atoms. The Fermi level has been set to zero matching the top of the valence band.

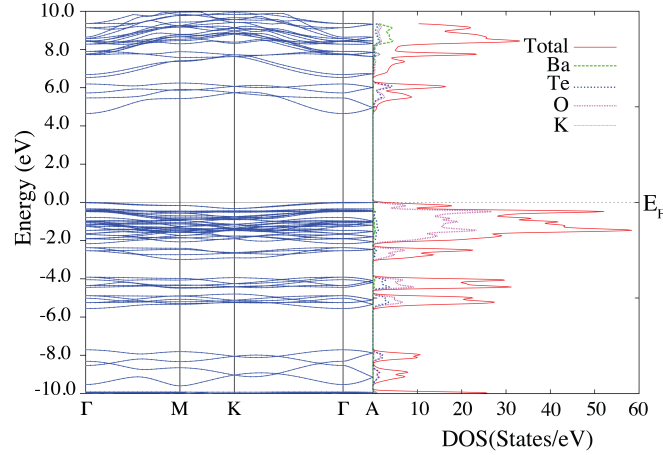


FIG. 4. Left panel: DFT/HSE computed electronic band dispersion of $\text{Ba}_2\text{K}_2\text{Te}_2\text{O}_9$ crystal along high symmetry directions in the first Brillouin zone. Right panel: Total and partial densities of states for Ba, Te, O, and K atoms. The Fermi level has been set to zero matching the top of the valence band.

of the dielectric functions for the three crystals. Note that since the triple perovskite is hexagonal, $\epsilon_x = \epsilon_y \neq \epsilon_z$. Similarly, the absorption coefficient for waves polarized in the a-b plane differs from that for waves polarized in the c-direction. The peaks in the absorption spectra and the imaginary part of the dielectric function result from transitions from O- $2p$ orbitals in the valence band to Zr- $4d$ orbitals in BaZrO_3 or to Te- $5s$ orbitals in BaCaTeO_6

TABLE I. Calculated bandgaps using PBE and HSE06 potentials, and hole trapping energy E_{ST}

Crystal	PBE bandgap (eV)	HSE06 bandgap (eV)	Bandgap type	E_{ST} (eV)
BaZrO ₃	2.94	4.90	Indirect	0.247
Ba ₂ CaTeO ₆	3.43	5.24	Direct	0.256
Ba ₂ K ₂ Te ₂ O ₉	2.88	4.65	Direct	0.248

and Ba₂K₂Te₂O₉.

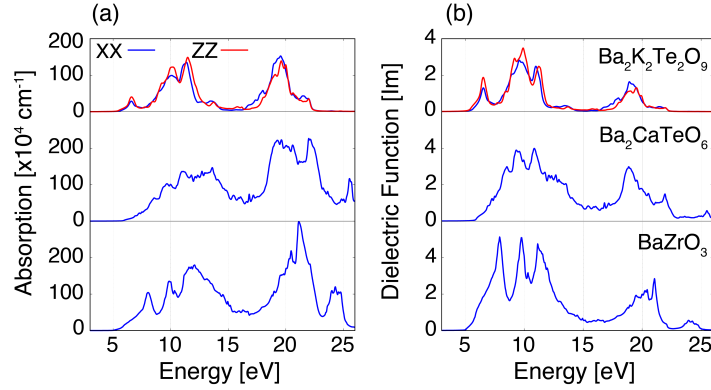


FIG. 5. (a) Optical absorption and (b) Imaginary part of the dielectric function computed from hybrid functionals for Ba₂K₂Te₂O₉ (top), Ba₂CaTeO₆ (middle) and BaZrO₃ (bottom). Note that Ba₂K₂Te₂O₉ has a hexagonal structure, hence the X and Z components of the absorption coefficient and dielectric function are not equal.

To calculate the hole self-trapping energy, an electron is removed from the supercell and the total energy E_1 is calculated using hybrid-functional density functional theory. Removal of an electron from the perfect supercell results in a delocalized hole at the valence band maximum. Next, atoms surrounding a certain oxygen atom are given random displacements, the atomic positions are relaxed, and the total energy E_2 is calculated. An energy E_2 lower than E_1 indicates that the hole is self-trapped; $E_1 - E_2$ would then correspond to the hole self-trapping energy. In all three crystals, we find that the hole is stabilized by small lattice distortion around an oxygen atom. In Table I we report the hole self-trapping energy for each of the perovskites considered in this work. Self-trapping of holes points to the difficulty of achieving p-type doping in these materials unless techniques similar to those employed by Pandey *et al.*¹⁰ are implemented.

To summarize, in this letter we studied the electronic and optic features of three barium-

based perovskites from first principles calculations based on hybrid functionals. Two of them, $\text{Ba}_2\text{CaTeO}_6$ and $\text{Ba}_2\text{K}_2\text{Te}_2\text{O}_9$, are proposed as novel ultrawide bandgap semiconductors with bandgaps of 5.24 eV and 4.65 eV, respectively. Contrary to ideal perovskites where the bandgap exhibit an indirect transition from R in the valance band to Γ in the conduction band²⁵, we find that the double and triple perovskites show a direct bandgap transition at the Γ -point. Similarly to other well established UWBG semiconductors, we predict that hole self-trapping is favorable through lattice distortions near oxygen sites. We hope that this work is viewed as a proof of concept and that it would encourage further experimental and theoretical investigations into perovskites as UWBG semiconductors, especially those exhibiting double and triple perovskite structures which have not been widely studied.

ACKNOWLEDGMENTS

This work was supported in part by the National Science Foundation under PREM grant no. DMR-1523588 and CREST grant no. HRD-1547723.

The data that support the findings of this study are available from the corresponding author upon reasonable request

REFERENCES

- ¹H. Kroemer, “Nobel lecture: Quasielectric fields and band offsets: teaching electrons new tricks,” *Rev. Mod. Phys.* **73**, 783–793 (2001).
- ²J. Y. Tsao, J. Han, R. H. Haitz, and P. M. Pattison, “The blue led nobel prize: Historical context, current scientific understanding, human benefit,” *Annalen der Physik* **527**, A53–A61 (2015), <https://onlinelibrary.wiley.com/doi/pdf/10.1002/andp.201570058>.
- ³S. Nakamura and M. R. Krames, “History of galliumnitride-based light-emitting diodes for illumination,” *Proceedings of the IEEE* **101**, 2211–2220 (2013).
- ⁴R. Haitz and J. Y. Tsao, “Solid-state lighting: The case 10 years after and future prospects,” *physica status solidi (a)* **208**, 17–29 (2011), <https://onlinelibrary.wiley.com/doi/pdf/10.1002/pssa.201026349>.
- ⁵J. Y. Tsao, S. Chowdhury, M. A. Hollis, D. Jena, N. M. Johnson, K. A. Jones, R. J. Kaplar, S. Rajan, C. G. Van de Walle, E. Bellotti, C. L. Chua, R. Collazo, M. E. Coltrin, J. A.

- Cooper, K. R. Evans, S. Graham, T. A. Grotjohn, E. R. Heller, M. Higashiwaki, M. S. Islam, P. W. Juodawlkis, M. A. Khan, A. D. Koehler, J. H. Leach, U. K. Mishra, R. J. Nemanich, R. C. N. Pilawa-Podgurski, J. B. Shealy, Z. Sitar, M. J. Tadjer, A. F. Witulski, M. Wraback, and J. A. Simmons, “Ultrawide-bandgap semiconductors: Research opportunities and challenges,” *Advanced Electronic Materials* **4**, 1600501 (2018).
- ⁶B. J. Baliga, “Semiconductors for highvoltage, vertical channel fieldeffect transistors,” *Journal of Applied Physics* **53**, 1759–1764 (1982), <https://doi.org/10.1063/1.331646>.
- ⁷E. Johnson, *RCA Review* , 263 (1965).
- ⁸J. B. Varley, A. Janotti, C. Franchini, and C. G. Van de Walle, “Role of self-trapping in luminescence and p -type conductivity of wide-band-gap oxides,” *Phys. Rev. B* **85**, 081109 (2012).
- ⁹W. Traiwattanapong, A. Janotti, N. Umezawa, S. Limpijumnong, J. T-Thienprasert, and P. Reunchan, “Self-trapped holes in batio3,” *Journal of Applied Physics* **124**, 085703 (2018).
- ¹⁰A. Pandey, X. Liu, Z. Deng, W. J. Shin, D. A. Laleyan, K. Mashooq, E. T. Reid, E. Kioupakis, P. Bhattacharya, and Z. Mi, “Enhanced doping efficiency of ultrawide band gap semiconductors by metal-semiconductor junction assisted epitaxy,” *Phys. Rev. Materials* **3**, 053401 (2019).
- ¹¹Z. Galazka, D. Klimm, K. Irmscher, R. Uecker, M. Pietsch, R. Bertram, M. Naumann, M. Albrecht, A. Kwasniewski, R. Schewski, and M. Bickermann, “Mgga2o4 as a new wide bandgap transparent semiconducting oxide: growth and properties of bulk single crystals,” *physica status solidi (a)* **212**, 1455–1460 (2015), <https://onlinelibrary.wiley.com/doi/pdf/10.1002/pssa.201431835>.
- ¹²E. Chikoidze, C. Sartel, I. Madaci, H. Mohamed, C. Vilar, B. Ballesteros, F. Belarre, E. del Corro, P. Vales-Castro, G. Sauthier, L. Li, M. Jennings, V. Sallet, Y. Dumont, and A. Prez-Toms, “ p -type ultrawide-band-gap spinel zn_{ga}2o₄: New perspectives for energy electronics,” *Crystal Growth & Design* **20**, 2535–2546 (2020).
- ¹³T. Endo, Y. Sato, H. Takizawa, and M. Shimada, “High-pressure synthesis of new compounds, ZnSiN₂ and ZnGeN₂ with distorted wurtzite structure,” *Journal of Materials Science Letters* **11**, 424–426 (1992).
- ¹⁴R. Jinno, C. S. Chang, T. Onuma, Y. Cho, S.-T. Ho, M. C. Cao, K. Lee, V. Protasenko, D. G. Schlom, D. A. Muller, H. G. Xing, and D. Jena, “Crystal orientation dictated epitaxy

- of ultrawide bandgap 5.4-8.6 eV α -(AlGa) $_2$ O $_3$ on m-plane sapphire,” [arXiv \(2020\)](#).
- ¹⁵Z. Y. A. Balushi, K. Wang, R. K. Ghosh, R. A. Vil, S. M. Eichfeld, J. D. Caldwell, X. Qin, Y.-C. Lin, P. A. DeSario, G. Stone, S. Subramanian, D. F. Paul, R. M. Wallace, S. Datta, J. M. Redwing, and J. A. Robinson, “Two-dimensional gallium nitride realized via graphene encapsulation,” [Nature Materials](#) **15**, 1166–1171 (2016).
 - ¹⁶I. Levin, T. G. Amos, S. M. Bell, L. Farber, T. A. Vanderah, R. S. Roth, and B. H. Toby, “Phase equilibria, crystal structures, and dielectric anomaly in the $\text{Ba}_2\text{Ca}_2\text{Zr}_2\text{O}_{10}$ system,” [Journal of Solid State Chemistry](#) **175**, 170 – 181 (2003).
 - ¹⁷W. Fu, Y. Au, S. Akerboom, and D. IJdo, “Crystal structures and chemistry of double perovskites $\text{Ba}_2\text{M}(\text{II})\text{M}'(\text{VI})\text{O}_6$ ($\text{M}=\text{Ca, Sr, M}'=\text{Te, W, U}$),” [Journal of Solid State Chemistry](#) **181**, 2523 – 2529 (2008).
 - ¹⁸M. Weil, “Crystal structures of the triple perovskites $\text{Ba}_2\text{K}_2\text{Te}_2\text{O}_9$ and $\text{Ba}_2\text{KNaTe}_2\text{O}_9$, and redetermination of the double perovskite $\text{Ba}_2\text{CaTeO}_6$,” [Acta Crystallographica Section E](#) **74**, 1006–1009 (2018).
 - ¹⁹P. Blaha, K. Schwarz, G. Madsen, D. Kvasnicka, J. Luitz, R. Laskowski, F. Tran, L. Marks, and L. Marks, [WIEN2k: An Augmented Plane Wave Plus Local Orbitals Program for Calculating Crystal Properties](#) (Techn. Universitat, 2019).
 - ²⁰J. Heyd, G. E. Scuseria, and M. Ernzerhof, “Hybrid functionals based on a screened coulomb potential,” [The Journal of Chemical Physics](#) **118**, 8207–8215 (2003).
 - ²¹G. Kresse and J. Furthmüller, “Efficient iterative schemes for ab initio total-energy calculations using a plane-wave basis set,” [Phys. Rev. B](#) **54**, 11169–11186 (1996).
 - ²²J. P. Perdew, K. Burke, and M. Ernzerhof, “Generalized gradient approximation made simple,” [Phys. Rev. Lett.](#) **77**, 3865–3868 (1996).
 - ²³X. Chen, J. Wang, C. Huang, S. Zhang, H. Zhang, Z. Li, and Z. Zou, “Barium zirconate: a new photocatalyst for converting CO_2 into hydrocarbons under UV irradiation,” [Catal. Sci. Technol.](#) **5**, 1758–1763 (2015).
 - ²⁴J. Robertson, “Band offsets of wide-band-gap oxides and implications for future electronic devices,” [Journal of Vacuum Science & Technology B: Microelectronics and Nanometer Structures Processing, Measurement, and Phenomena](#) **18**, 1785–1791 (2000).
 - ²⁵S. Krübel, M. A. L. Marques, and S. Botti, “Stability and electronic properties of new inorganic perovskites from high-throughput ab initio calculations,” [J. Mater. Chem. C](#) **4**, 3157–3167 (2016).